Eur. Phys. J. A **11**, 105–111 (2001)

THE EUROPEAN PHYSICAL JOURNAL A

The role of hyperon resonances in $p(\gamma, K^+)\Lambda$ processes

S. Janssen[a], J. Ryckebusch[b], W. Van Nespen, D. Debruyne, and T. Van Cauteren

Department of Subatomic and Radiation Physics, Ghent University, Proeftuinstraat 86, B-9000 Gent, Belgium

Received: 8 February 2001 / Revised version: 19 April 2001
Communicated by Th. Walcher

Abstract. We discuss the role of hyperon resonances in the u-channel when modeling $p\,(\gamma, K^+)\,\Lambda$ processes in an effective Lagrangian approach. Without the introduction of hyperon resonances, one is forced to use soft hadronic form factors with a cutoff mass which is at best two times the kaon mass. After inclusion of the hyperon resonances in the u-channel, we obtain a fair description of the data with a cutoff mass of the order of 1.8 GeV.

PACS. 13.60.Le Meson production – 14.20.Jn Hyperons – 14.20.Gk Baryon resonances with $S = 0$

1 Introduction

Photo-production of strangeness on the nucleon is a potentially powerful tool for studying hadrons at the "constituent-quark" scale of ~ 1 GeV [1]. It is hoped that through comparing model calculations with sufficiently large sets of $p\,(\gamma, K^+)\,\Lambda$ data [2], our understanding of the excitation spectrum and the structure of the nucleon will be deepened. Regarding our knowledge about the excitation spectrum of the nucleon, strangeness production provides a study domain for resonances which remain undiscovered in π photo-production or $\pi N \to \pi N$ scattering reactions. At variance with the (γ, π) reaction, even at threshold, the invariant energy of the $p\,(\gamma, K^+)\,\Lambda$ reaction exceeds the mass of several hadron resonances. Accordingly, in modeling $p\,(\gamma, K^+)\,\Lambda$ processes in terms of hadronic degrees of freedom, a considerable part of the excitation spectrum of the nucleon can in principle participate in the reaction mechanism. For some of these resonances, the existence and branching into the strange channels is well established. For others, no convincing empirical evidence in support of their existence could as yet be produced. When calculating $p\,(\gamma, K^+)\,\Lambda$ observables within the framework of effective field theories, one frequently employs various combinations of hadron resonances. This procedure may be perceived as cooking an effective model in which resonances are brought in and thrown away until a specific set fits the data. Several calculations, however, have shown that the data cannot be reproduced without including some particular resonances, thereby providing indirect support for the existence of these excited states and their branching into the strange channels.

Apart from the choices with respect to the intermediate hadronic states, an effective Lagrangian approach for the $p\,(\gamma, K^+)\,\Lambda$ reaction involves the introduction of a set of coupling constants. Being parameters in an effective theory, these coupling constants can be calculated on the basis of QCD-inspired constituent-quark models for the hadrons [3,4]. In this manner, the link between the $p\,(\gamma, K^+)\,\Lambda$ data and the quark models for baryons is established. Accordingly, the effective field theories allow to test theoretical predictions for coupling constants against photo-production data.

Despite their success in reproducing the $p\,(\gamma, K^+)\,\Lambda$ observables over a photo-energy range from threshold up to roughly 2 GeV, the hadronic models are facing a number of difficulties. First, at photon lab energies above 2 GeV, the predictions of all isobar models tend to overestimate the measured cross-sections. This feature is partly caused by t-channel processes [5]. Another difficulty is less well known and concerns the fact that the Born terms in their own predict $p\,(\gamma, K^+)\,\Lambda$ cross-sections which are a few times the measured ones. In this paper, we discuss various methods for counterbalancing the strength produced by these Born terms. It turns out that hyperon resonances can provide a natural mechanism to produce theoretical cross-sections of the right order of magnitude.

The outline of this paper is as follows. In sect. 2 the isobar model for K^+ photo-production on the proton is briefly reviewed. In sect. 3 the results of our numerical $p(\gamma, K^+)\Lambda$ calculations are presented and the contribution from the different terms in the reaction dynamics detailed. Our conclusions are presented in sect. 4.

2 The isobar model

Since the early work of Thom [6] in the mid sixties, great effort has been put into developing an isobar (or, hadronic) model for the description of $p\,(\gamma, K^+)\,\Lambda$ processes [7–12].

[a] e-mail: stijn.janssen@rug.ac.be
[b] e-mail: jan.ryckebusch@rug.ac.be

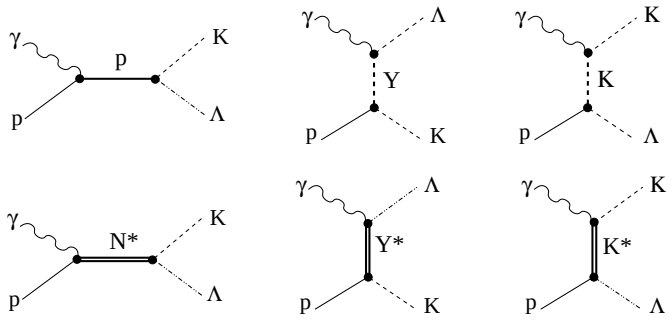

Fig. 1. Diagrams contributing to the $p(\gamma, K^+)\Lambda$ process at the tree level. The upper row corresponds to the Born terms in which a proton is exchanged in the s-channel, a Λ or Σ^0 in the u-channel and a K^+ in the t-channel. The lower row shows the corresponding diagrams with the exchange of an excited particle or resonance.

Essentially, these effective field theories provide propagators for the intermediate particles and the structure of the interaction Lagrangians describing the strong and electromagnetic vertices. With this input one can compute the Feynman amplitudes $\mathcal{M}_{\lambda}^{\lambda_1\lambda_2}$ for a $p(\lambda_1) + \gamma(\lambda) \longrightarrow K^+ + \Lambda(\lambda_2)$ process which determines the differential cross-section (in the center-of-mass frame) through the following relation:

$$\frac{\mathrm{d}\sigma}{\mathrm{d}\Omega} = \frac{1}{64\pi^2}\frac{|\mathbf{p}_K|}{\omega}\frac{1}{W^2}\frac{1}{4}\sum_{\lambda_1\lambda_2\lambda}\left|\mathcal{M}_{\lambda}^{\lambda_1\lambda_2}\right|^2 , \qquad (1)$$

with λ_1, λ_2 and λ respectively denoting the nucleon, hyperon and photon polarization. Further, $W \equiv \sqrt{s}$ is the invariant energy of the reaction. At the tree level, the Feynman amplitude is completely determined by the diagrams contained in fig. 1. Here, we discriminate between the diagrams that have hadrons in their ground state $(p, \Lambda, \Sigma^0, K)$ and those that have hadron resonances $(N^*,\ \Lambda^*,\ \Sigma^*,\ K^*)$ in the reaction path. In the isobar model, the composite nature of the hadrons is accounted for through the introduction of form factors at every hadronic vertex. A widely used form for these hadronic form factors is [13,14]

$$F_x(\Lambda) = \frac{\Lambda^4}{\Lambda^4 + (x - M^2)^2} \qquad (x \equiv s, t, u) , \qquad (2)$$

where x is the corresponding Mandelstam variable of the diagram in question. Further, Λ is a cutoff parameter. This cutoff parameter sets a short-distance scale beyond which the hadronic model is conceived to fail. At best, the hadronic form factors may provide a completely phenomenological description of the dynamical processes which occur at distances smaller than those determined by the parameter Λ. For the sake of minimizing the number of free parameters, we introduce one cutoff parameter for the hadronic vertices in the various Born terms (diagrams in the upper row of fig. 1) and one for all the resonant terms (diagrams in the lower row of fig. 1). To restore the broken gauge invariance after introducing hadronic form factors, we adopt[1] a procedure suggested by Haberzettl *et al.* [13].

Table 1. Overall agreement between the model calculations and the SAPHIR data for the different sets of resonances and cutoff masses. We denote by "basic set" the following set of intermediate particles: $K^*, K_1, N^*_{1650}, N^*_{1710}, N^*_{1720}$.

Resonance set	Λ (GeV)	χ^2
basic set	≥ 1.6	10.32
basic set	≥ 0.4	4.36
basic set + N^*_{1895}	≥ 1.6	7.38
basic set + N^*_{1895}	≥ 0.4	2.64
basic set + Λ^*_{1800} Λ^*_{1810}	≥ 1.6	3.43
basic set + N^*_{1895} Λ^*_{1800} Λ^*_{1810}	≥ 1.6	2.65

We have developed a computer program for the calculation of the strangeness production observables. With the aid of a symbolic trace calculation, we first evaluate the expression for $\left|\mathcal{M}_{\lambda}^{\lambda_1\lambda_2}\right|^2$ for the most general case of pseudoscalar meson photo-production. Hereby, intermediate vector mesons and baryons with $J = \frac{1}{2}$ and $\frac{3}{2}$ can be accommodated. Second, the observables for $p(\gamma, K^+)\Lambda$ are computed numerically starting from the general expression for $\left|\mathcal{M}_{\lambda}^{\lambda_1\lambda_2}\right|^2$ and specific choices with respect to intermediate particles, coupling constants and cutoff masses. A detailed outline of our model will be presented in a forthcoming paper [16].

3 Results and discussion

As mentioned in the introduction, at present it is not clear which resonances represent the major contributions to the $p(\gamma, K^+)\Lambda$ reaction mechanism. From a kinematical point of view, there are more than twenty likely candidates. Over the years, several combinations of resonances have been proposed in literature [7–11]. In all cases, good agreement with the available data was achieved although the conclusions and suggested sets of resonances were not unambiguous. This diversity shows the complexity of the process and proves that after more than three decades of research, there is still no established reaction mechanism for the $p(\gamma, K^+)\Lambda$ process.

In our choice with respect to the intermediate particles, we have, in a first step, been guided by a recent coupled-channel analysis [17] that recognized the importance of three intermediate states: two spin-(1/2) nucleon resonances ($N^*(1650)$ and $N^*(1710)$) and one spin-(3/2) nucleon resonance ($N^*(1720)$). Note that these nucleon

[1] After the completion of the numerical calculations that led to this work, Davidson and Workman [15] criticized some aspects of the procedure of Haberzettl and suggested a different form factor for the gauge breaking terms.

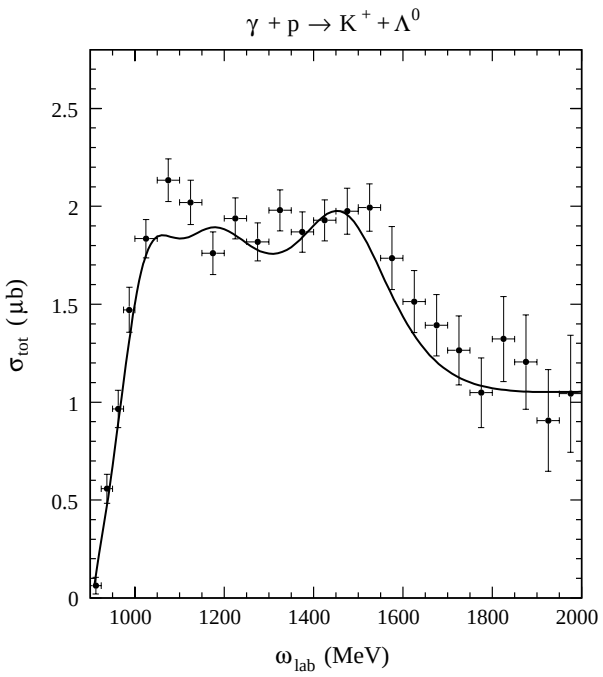

Fig. 2. Our calculated result for the total cross-section in a model which includes the resonances K^*, K_1, N^*_{1650}, N^*_{1710}, N^*_{1720} and N^*_{1895} and uses a soft cutoff mass $\Lambda \sim 0.42$ GeV. The data are from ref. [2].

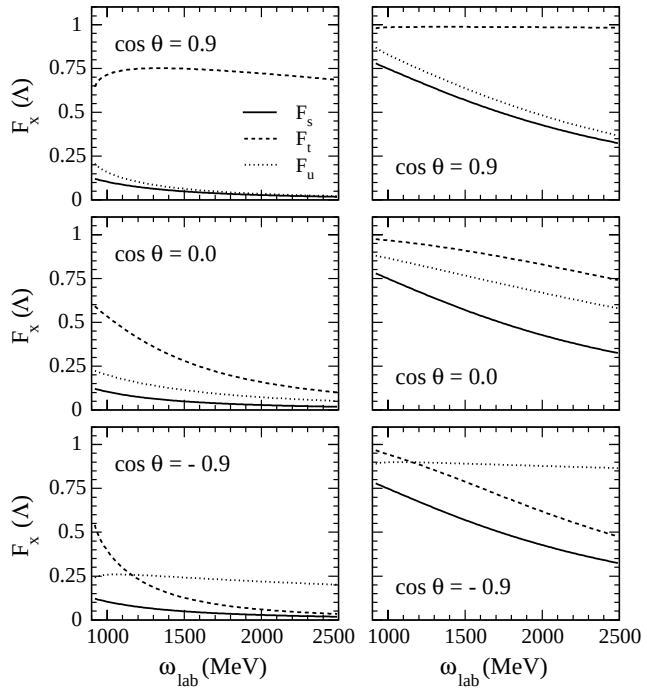

Fig. 3. The hadronic form factors $F_x(\Lambda)$ for two values of the cutoff mass and for three kaon angles. For the left panels $\Lambda = 0.8$ GeV, for the right panels $\Lambda = 1.8$ GeV. The solid line shows $F_s(\Lambda)$, the dashed line $F_t(\Lambda)$ and the dotted line $F_u(\Lambda)$.

resonances are also the only ones in the particle data tables [18] with significant branching into the strange channels. At higher energies [2], the $p(\gamma, K^+)\Lambda$ data exhibit a typical diffractive nature. It is well known that this feature is mainly due to t-channel processes. For this reason, the two lowest vector meson resonances ($K^*(892)$ and $K_1(1270)$) are also explicitly included in our model calculations. These five resonances (N^*_{1650}, N^*_{1710}, N^*_{1720}, K^* and K_1) constitute the basis of our reaction dynamics. Nevertheless, an attempt to fit the cross-section and polarization data with this basic set of five intermediate particles, was only reasonably successful. Indeed, the agreement did not get any better than $\chi^2 \sim 10.32$ (see table 1). This χ^2 expresses the conformity of the model calculations to the data. A value of 10.32 indicates that there is room for other resonances as intermediate particles beyond the basic set of five.

The research in this field has experienced a new impulse with the advent of the $p(\gamma, K^+)\Lambda$ data from the SAPHIR experiment at Bonn [2]. These data provide some indications for a structure in the $p\,(\gamma, K^+)\,\Lambda$ total cross-section about $\omega_{\rm lab} = 1500$ MeV. Due to limited energy resolution and statistics, this structure could not be revealed in previous experiments. Recently, the Washington group [12] pointed out that model calculations could account for this structure after including an additional spin-(3/2) nucleon resonance N^*_{1895} in the s-channel. The existence of this D_{13} resonance with considerable branching into the strange channel, was predicted by the constituent-quark model calculations of Capstick and Roberts [19]. Therefore, the authors of ref. [12] legitimately claimed support for the existence of one of the "missing resonances". Our calculations confirm the conclusions drawn by the Washington group. When including the N^*_{1895} in addition to the basic set of five intermediate particles, we arrive at a promising $\chi^2 \sim 2.64$ (see table 1). The computed total cross-section as a function of the photon lab energy is given in fig. 2.

At this point, it is worth stressing that the quality of agreement between the model calculations and the data very much depends on the adopted value of the cutoff mass Λ for the Born terms. As is mostly done, the cutoff mass is treated as a free parameter. First, we considered the case where Λ was allowed to vary freely imposing an underlimit of 0.4 GeV, though. The best fit was reached with a value $\Lambda \sim 0.42$ GeV, which corresponds to a soft form factor. We also considered the case where we forced the cutoff mass to be larger than 1.6 GeV, which corresponds to a pronounced "hard" form factor. With the hard form factor, the overall agreement with the data was inferior ($\chi^2 \sim 7.38$) to what was achieved ($\chi^2 \sim 2.64$) with the same set of intermediate particles (basic set extended with N^*_{1895}) but with a freely varying value of Λ. From these observations, it is clear that the hadronic form factors play a crucial role in the reaction dynamics.

We now attempt to figure out why the model with five or six intermediate particles does a much better job in reproducing the data, when soft hadronic form factors are used. To that purpose, we separate the amplitude in so-called non-resonant parts represented by the Born terms (upper row in fig. 1) and resonant parts, where resonances

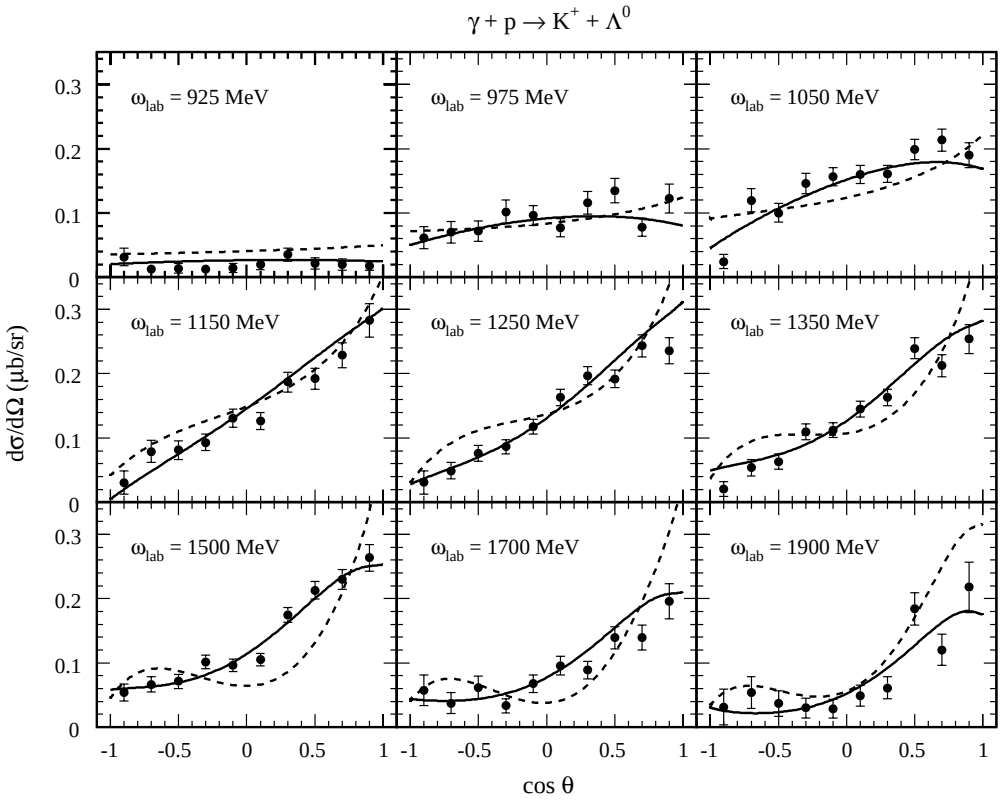

Fig. 4. Model calculations for the differential cross-section at various photon energies. The dashed curves represent a calculation with the "basic set + N^*_{1895}". For the solid curves this set was extended with two hyperon resonances (Λ^*_{1800} and Λ^*_{1810}). A hard form factor ($\Lambda \geq 1.6$ GeV) is used in both model calculations. The data are from the SAPHIR collaboration [2].

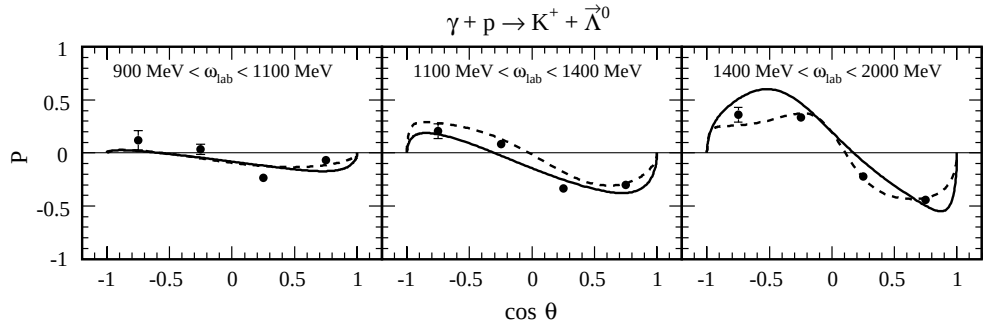

Fig. 5. Model calculations for the recoil polarization asymmetry at various photon energies. The curves are as in fig. 4. The data are from the SAPHIR collaboration [2].

are the intermediate particles (lower row in fig. 1). The non-resonant terms introduce two free parameters in the form of the coupling constants $g_{\Lambda Kp}$ and $g_{\Sigma^0 Kp}$. Imposing $SU(3)$ flavor symmetry, these coupling constants can be related to the pion nucleon coupling strength $g_{\pi NN}$. Despite the fact that $SU(3)$ is a broken symmetry, these relations can be used to impose a range of values for the two coupling constants. Assuming that the symmetry is broken at the level of 20%, ranges are

$$\begin{aligned} -4.5 \;\leq\; g_{\Lambda Kp}/\sqrt{4\pi} \;\leq\; -3.0\,, \\ 0.9 \;\leq\; g_{\Sigma^0 Kp}/\sqrt{4\pi} \;\leq\; 1.3\,. \end{aligned} \tag{3}$$

With values of $g_{\Lambda Kp}$ and $g_{\Sigma^0 Kp}$ in these ranges, the non-resonant terms are observed to produce an amount of strength which is at least a factor of 4 or 5 larger than the measured cross-sections. There are a number of solutions to resolve this problem. One possibility is to let the coupling constants adopt values beyond the $SU(3)$ limits. In practice, this amounts to reducing $g_{\Lambda Kp}$ and $g_{\Sigma^0 Kp}$ to (absolute) values far smaller than what is expected within (broken) $SU(3)$ [11]. Another possibility is the introduction of a resonant term that interferes destructively with the non-resonant contribution. A third possibility, adopted by the Washington group [13], is the

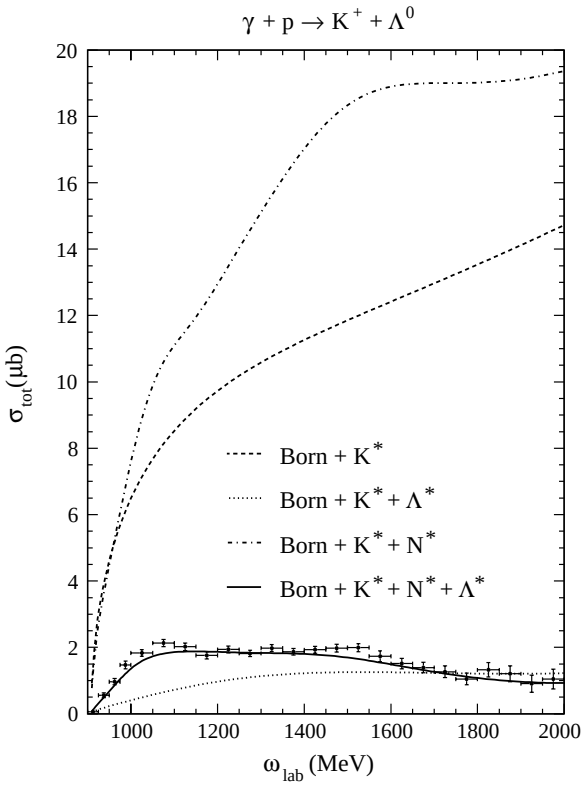

Fig. 6. The total $p(\gamma, K^+)\Lambda$ cross-section as a function of the photon lab energy. The dashed line gives the combined Born and vector meson strength, the dot-dashed line includes in addition nucleon resonances in the s-channel. The dotted curve shows the effect of including hyperon resonances to the Born and vector meson background. The solid line is a calculation with the complete set. The cutoff mass in these model calculations was $\Lambda \sim 1.78$ GeV.

introduction of a soft hadronic form factor for the non-resonant terms. The sensitivity of the hadronic form factor to the value of Λ is illustrated in fig. 3 for a few values of the kaon center-of-mass angle θ.

As can be inferred from comparing the left and right panels in fig. 3, the introduction of soft hadronic form factors induces a severe reduction of the strength attributed to the Born terms. As a consequence, when the cutoff mass is chosen sufficiently low, the coupling constants can be kept between their $SU(3)$ limits and there is no need for an extra resonant term to counterbalance the strength from the Born diagrams. It appears, however, that the cutoff masses at which the strength from the non-resonant terms can be sufficiently suppressed, are of the order of the kaon mass. These small values of Λ may raise some questions with respect to the realistic character and applicability of the "effective" theory. Indeed, as mentioned above, the value of the cutoff mass sets a short-distance scale to the theory and we believe that a $\Lambda = 0.8$ GeV is probably already an under-limit of what appears to be a reasonable cutoff mass. Moreover, the severe reduction of the Born strength through the introduction of a soft form factor (see fig. 3) may appear as a rather artificial way of keeping $g_{\Lambda Kp}$ and $g_{\Sigma^0 Kp}$ in agreement with the $SU(3)$ expectations.

A value of $\Lambda \sim m_K$ also appears to be rather small in comparison with the typical values which are predicted in potential models for the hadron forces. For example, the values for Λ quoted by the Nijmegen [20] and the Jülich group [21] are close to 1.2 GeV. Recently, the Jülich group [22] even proposed cutoff masses in the meson-baryon sector exceeding 2 GeV.

Here, we suggest an alternative method to counterbalance the unrealistically large amounts of strength produced by the non-resonant Born diagrams. We find that, after the inclusion of the two spin-(1/2) hyperon resonances $\Lambda^*(1800)$ and $\Lambda^*(1810)$ (both received a $(***)$-ranking by the Particle Data Group [18]) in the u-channel, the overall χ^2 for the complete data set drops from 7.38 to 2.65 (see table 1). This agreement with the data is as favorable as the one obtained with the "basic set + N^*_{1895}" in combination with a soft hadronic form factor. We observe that after including the hyperon resonances, good fits to the data were achieved with hard form factors corresponding with typical values of $\Lambda \sim 1.8$ GeV. The coupling strengths of these two intermediate Λ^* states turns out to be relatively large in comparison with the typical values obtained for the nucleon resonances couplings. We have also tried other combinations of known spin-(1/2) hyperon resonances in the u-channel. All combinations improved the global agreement between the calculations and the complete data set. Furthermore, in all cases a similar qualitative interference pattern between the other terms was observed. The combination of Λ^*_{1800} and Λ^*_{1810}, though, produced the best χ^2. *Therefore, the suggested procedure of including hyperon resonances in the u-channel emerges as a natural way of compensating for the strength produced by the Born terms and allows the cutoff masses to have more realistic values.*

As illustrated in fig. 4 and fig. 5, after inclusion of the hyperon resonances in the reaction dynamics, a fair agreement between the calculations and the data is reached ($\chi^2 \sim 2.65$). Admittedly, although the N^*_{1895} is explicitly included, the calculations (solid line in fig. 6) do not longer predict a pronounced structure in the total cross-section about $\omega_{\rm lab} = 1500$ MeV.

The origin of the successes achieved with the introduction of hyperon resonances can be traced back to a strong destructive interference between the contribution from the hyperon resonances and the Born terms. This can be inferred from a detailed examination of fig. 6 which shows the contributions to the total cross-section from the different types of resonances (vector meson resonances $K^* \equiv (K^*, K_1)$, nucleon resonances $N^* \equiv (N^*_{1650}, N^*_{1710}, N^*_{1720}, N^*_{1895})$, and hyperon resonances $\Lambda^* \equiv (\Lambda^*_{1800}, \Lambda^*_{1810})$). It should be stressed that the different curves do not represent the best fit to the data for a particular combination of intermediate particles. The curves show the predicted strength from a specific combination of diagrams, when fixing the parameters with values that are obtained in a calculation that includes the "basic set + N^*_{1895}, Λ^*_{1800}, Λ^*_{1810}". So, the different curves in fig. 6 illustrate how

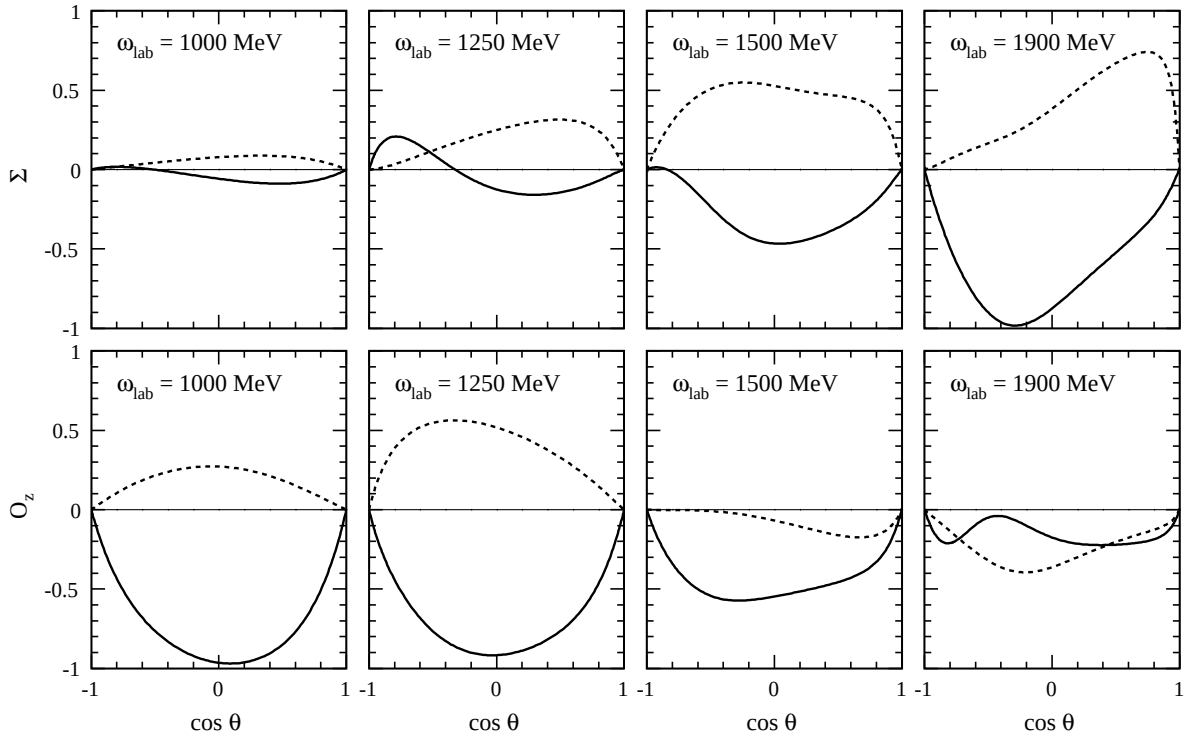

Fig. 7. Model predictions for the photon polarization asymmetry Σ and the double polarization beam-recoil asymmetry O_z at various photon lab energies. The dashed curves are calculations for the "basic set + N^*_{1895}" and a cutoff mass $\Lambda \sim 0.42$ GeV. The solid curves are calculations where the same set is extended with Λ^*_{1800} and Λ^*_{1810} and a cutoff mass $\Lambda \sim 1.78$ GeV.

the final result (solid curve) comes about as a coherent sum of several contributing diagrams. The combination of Born terms (with coupling constants constrained within the $SU(3)$ ranges of eq. (3)) and vector mesons produces far too much strength in comparison with the measured cross-sections. After including the hyperon resonances (denoted by "Born $+K^* + \Lambda^*$"), the computed cross-section has already the right order of magnitude due to a destructive interference. Further inclusion of the nucleon resonances in the s-channel produces the required structure of the cross-section but does not sizably alter the magnitudes. Including all terms but the Λ^*'s in the u-channel (a calculation denoted by "Born $+K^* + N^*$") we obtain cross-sections that overshoot the data by almost an order of magnitude. Concluding, it is essential to realize that hyperons in the u-channel are likely candidates for playing a predominant role in the $p(\gamma, K^+)\Lambda$ reaction dynamics.

We summarize our findings in table 1, where we give an overview of the best χ^2 values which we achieved for the various combinations of resonances. For these calculations we have used all the SAPHIR data, including the complete set of total and differential cross-sections and recoil polarization asymmetries. Without the introduction of a hyperon resonance in the reaction dynamics, a soft hadronic form factor produces a far better description of the data than a hard one. A χ^2 calculation with the basic set of five intermediate particles ($K^*, K_1, N^*_{1650}, N^*_{1710}, N^*_{1720}$) improves from 10.32 to 4.36 when a soft instead of a hard hadronic form factor is used. In both cases (hard and soft cutoff masses) the χ^2 further decreases after adding the "missing" N^*_{1895} resonance to the basic set ($\chi^2 = 7.38$ for $\Lambda \geq 1.6$ GeV, $\chi^2 = 2.64$ for $\Lambda \geq 0.4$ GeV). One way of obtaining reasonable fits with hard hadronic form factors is allowing hyperon resonances in the reaction dynamics.

Inspecting table 1, one observes that after implementing hyperon resonances in the reaction dynamics, the supplementary introduction of the N^*_{1895} does only lead to a minor improvement in the quality of the description of the data, despite the fact that 5 additional parameters are introduced in the fitting procedure.

From the above discussion it becomes clear that as far as it comes to reproduce the differential cross-sections, the two approaches (soft hadronic form factors or hyperon resonances and hard hadronic form factors) produce comparable results. This is, however, not the case for all the observables. To illustrate this, we present model calculations for single and double polarization asymmetries. Figure 7 shows predictions for the photon polarization asymmetry Σ and the double beam-recoil asymmetry O_z. These quantities are defined as

$$\Sigma = \frac{\mathrm{d}\sigma/\mathrm{d}\Omega^{(\perp)} - \mathrm{d}\sigma/\mathrm{d}\Omega^{(\parallel)}}{\mathrm{d}\sigma/\mathrm{d}\Omega^{(\perp)} + \mathrm{d}\sigma/\mathrm{d}\Omega^{(\parallel)}}\,, \tag{4}$$

$$O_z = \frac{\mathrm{d}\sigma/\mathrm{d}\Omega^{(++)} - \mathrm{d}\sigma/\mathrm{d}\Omega^{(+-)}}{\mathrm{d}\sigma/\mathrm{d}\Omega^{(++)} + \mathrm{d}\sigma/\mathrm{d}\Omega^{(+-)}}\,. \tag{5}$$

In eq. (4) $\perp$ ($\parallel$) refers to linearly polarized photons perpendicular (parallel) to the reaction plane. In eq. (5) the first $+(-)$ corresponds with linearly polarized photons under an angle of $+(-)\pi/4$ with respect to the scattering

plane. The second $+(-)$ refers to recoil polarization parallel (anti parallel) to the momentum of the escaping Λ. In different energy regions, both observables seem to be extremely sensitive to the introduction of hyperon resonances and the magnitude of the adopted cutoff masses.

4 Conclusions

We have suggested an alternative technique to counterbalance the unreasonably high strength which is produced by the Born terms in effective-field approaches to the $\gamma + p \to K^+ + \Lambda$ process. It involves both the introduction of hyperon resonances in the u-channel and form factors at the hadronic vertices. Herewith, we obtain a fair description of the SAPHIR cross-sections and polarization observables with values of the hadronic cutoff mass that are a few times the kaon mass. Alternative approaches to counterbalance the strength from the Born terms, either go out from soft hadronic form factors with cutoff masses that are of the order of the kaon mass or use coupling constants smaller than those predicted by $SU(3)$ constraints. We have observed that the presence of the hyperon resonances in the u-channel has a large impact on the predicted values for the polarization observables. We believe that the measurement of these quantities could distinguish between the different models for the underlying dynamics of the strangeness production process and could shed light on the value of the cutoff masses.

This work was supported by the Fund for Scientific Research-Flanders under contract number 4.0061.99.

References

1. P. Geiger, N. Isgur, Phys. Rev. D **55**, 299 (1997).
2. M.Q. Tran *et al.*, Phys. Lett. B **445**, 20 (1998); `http://lisa12.physik.uni-bonn.de/saphir/klks.txt`.
3. S. Capstick, N. Isgur, Phys. Rev. D **34**, 2809 (1986).
4. S. Capstick, W. Roberts, Phys. Rev. D **49**, 4570 (1994).
5. M. Guidal, J.-M. Laget, M. Vanderhaeghen, Nucl. Phys. A **627**, 645 (1997).
6. H. Thom, Phys. Rev. **151**, 1322 (1966).
7. R. Adelseck, C. Bennhold, L. Wright, Phys. Rev. C **32**, 1681 (1985).
8. R. Adelseck, B. Saghai, Phys. Rev. C **42**, 108 (1990).
9. R. Williams, C.-R. Ji, S. Cotanch, Phys. Rev. C **46**, 1617 (1992).
10. J. David, C. Fayard, G. Lamot, B. Saghai, Phys. Rev. C **53**, 2613 (1996).
11. S. Hsiao, D. Lu, S. Yang, Phys. Rev. C **61**, 068201 (2000).
12. T. Mart, C. Bennhold, Phys. Rev. C **61**, (R)012201 (2000).
13. H. Haberzettl, C. Bennhold, T. Mart, T. Feuster, Phys. Rev. C **58**, (R)40 (1998).
14. B. Pearce, B. Jennings, Nucl. Phys. A **528**, 655 (1991).
15. R. Davidson, R. Workman, Phys. Rev. C **63**, 025210 (2001).
16. S. Janssen *et al.*, work in preparation.
17. T. Feuster, U. Mosel, Phys. Rev. C **59**, 460 (1999).
18. Particle Data Group, (D.E. Groom *et al.*), Eur. Phys. J. C **15**, 1 (2000).
19. S. Capstick, W. Roberts, Phys. Rev. D **58**, 074011 (1998).
20. T. A. Rijken, V. Stoks, Y. Yamamoto, Phys. Rev. C **59**, 21 (1999).
21. B. Holznkamp, K. Holinde, J. Speth, Nucl. Phys. A **500**, 485 (1989).
22. J. Haidenbauer, W. Melnitchouk, J. Speth, Nucl. Phys. A **663-664**, 549c (2000); nucl-th/9805014.